BMC Urology

RESEARCH

Open Access

# Prediction of T staging in PI-RADS 4–5 prostate cancer by combination of multiparametric MRI and $^{68}$Ga-PSMA-11 PET/CT

Yuanzhen Ding[1†], Chenghao Mo[2†], Qiubo Ding[1†], Tingsheng Lin[1], Jie Gao[1], Mengxia Chen[1], Wenfeng Lu[1], Jiyuan Sun[1], Feng Wang[3], Shiming Zang[3], Qing Zhang[1*], Shiwei Zhang[1*] and Hongqian Guo[1*]

## Abstract

**Background** In this study, we explored the diagnostic performances of multiparametric magnetic resonance imaging (mpMRI), $^{68}$ Ga-PSMA-11 PET/CT and combination of $^{68}$ Ga-PSMA-11 PET/CT and mpMRI (mpMRI + PET/CT) for extracapsular extension (ECE). Based on the analyses above, we tested the feasibility of using mpMRI + PET/CT results to predict T staging in prostate cancer patients.

**Methods** By enrolling 75 patients of prostate cancer with mpMRI and $^{68}$ Ga-PSMA-11 PET/CT before radical prostatectomy, we analyzed the detection performances of ECE in mpMRI, $^{68}$ Ga-PSMA-11 PET/CT and mpMRI + PET/CT on their lesion images matched with their pathological sample images layer by layer through receiver operating characteristics (ROC) analysis. By inputting the lesion data into Prostate Imaging Reporting and Data System (PI-RADS), we divided the lesions into different PI-RADS scores. The improvement of detecting ECE was analyzed by net reclassification improvement (NRI). The predictors for T staging were evaluated by using univariate and multivariable analysis. The Kappa test was used to evaluate the prediction ability.

**Results** One hundred three regions of lesion were identified from 75 patients. 50 of 103 regions were positive for ECE. The ECE diagnosis AUC of mpMRI + PET/CT is higher than that of mpMRI alone ($\Delta$AUC = 0.101; 95% CI, 0.0148 to 0.1860; $p < 0.05$, respectively). Compared to mpMRI, mpMRI + PET/CT has a significant improvement in detecting ECE in PI-RADS 4–5 (NRI 36.1%, $p < 0.01$). The diagnosis power of mpMRI + PET/CT was an independent predictor for T staging ($p < 0.001$) in logistic regression analysis. In patients with PI-RADS 4–5 lesions, 40 of 46 (87.0%) patients have correct T staging prediction from mpMRI + PET/CT ($\kappa$ 0.70, $p < 0.01$).

**Conclusion** The prediction of T staging in PI-RADS 4–5 prostate cancer patients by mpMRI + PET/CT had a quite good performance.

†Yuanzhen Ding, Chenghao Mo and Qiubo Ding contributed equally to this work.

*Correspondence:
Qing Zhang
drzhangq@nju.edu.cn
Shiwei Zhang
zsw999@hotmail.com
Hongqian Guo
dr.ghq@nju.edu.cn
Full list of author information is available at the end of the article

**Keywords** Prostate cancer, Multiparametric MRI, $^{68}$Ga-PSMA-11 PET/CT, T staging, Extracapsular extension

## Background

As prostate cancer has been the fourth most frequent cancer worldwide, there is an urgent need for an accurate primary staging method in order to perform better clinical management [1, 2]. Since $^{68}$ Ga-PSMA-11 PET/CT and multiparametric magnetic resonance imaging (mpMRI) both have a greater accuracy than conventional imaging, they may have a positive influence on primary staging and patient management for prostate cancer treatment [3, 4]. The combination of $^{68}$ Ga-PSMA-11 PET/CT and mpMRI (mpMRI + PET/CT) is able to improve the detection of clinically significant prostate cancer (csPCa), which means that more accurate initial diagnosis requires more sophisticated techniques [5].

TNM system (American Joint Committee on Cancer, AJCC) is the most widely used in prostate cancer staging [6]. According to the 8E AJCC, extracapsular extension (ECE) is in T3 [7]. ECE is the adverse risk factor and reference factor of primary staging for prostate cancer, hence their detection plays a vital role in planning surgical strategy and prognosis of patients [8–11]. Among the patients after radical prostatectomy, ECE might be the predictor of biochemical recurrence and shorter survival time [10, 12]. Nowadays, prediction models like nomograms are limited tools without medical imaging information to predict the risk of ECE. It's urgently needed to use more accurate diagnostic tools to detect ECE so that T staging of prostate cancer can be more accurately detected.

$^{68}$ Ga-PSMA-11 PET/CT is the $^{68}$ Ga labelled small molecular inhibitor PSMA-11 via the HBED chelator for imaging with positron emission tomography (PET) combined computed tomography (CT) [13, 14]. Nomenclature is in accordance with the International Consensus Radiochemistry Nomenclature Guidelines [15]. Initially, $^{68}$ Ga-PSMA-11 PET showed favorable sensitivity and specificity in the detection of metastases with biochemical recurrence in prostate cancer [16]. Afterwards, $^{68}$ Ga-PSMA-11 PET/CT also became the study instrument for primary diagnosis of prostate cancer and performed well [3, 5, 17]. However, the utility of $^{68}$ Ga-PSMA-11 PET/CT in primary staging and therapy planning of prostate cancer should be evaluated [18].

mpMRI has been reported to be able to mitigate the overdiagnosis or underdiagnosis via mpMRI-targeted biopsy, particularly for the csPCa [19, 20]. Moreover, mpMRI has high specificity for the local staging of prostate cancer including detection of ECE [21]. However, mpMRI has limited sensitivity and is more likely to detect large, solitary, aggressive tumors [21, 22].

This study was aimed at comparing the diagnostic accuracy among $^{68}$ Ga-PSMA-11 PET/CT, mpMRI and mpMRI + PET/CT for the detection of ECE on a consecutive cohort of patients with whole-mount prostate tissue. At last, the prediction of T staging by mpMRI + PET/CT was presented.

## Methods

### Participants

A total of 595 consecutive patients of prostate cancer who had undergone 3.0 T mpMRI between March 2017 and December 2019 were retrospectively identified. We excluded the patients with these features as followed: (a) no $^{68}$ Ga-PSMA-11 PET/CT within 3 months; (b)

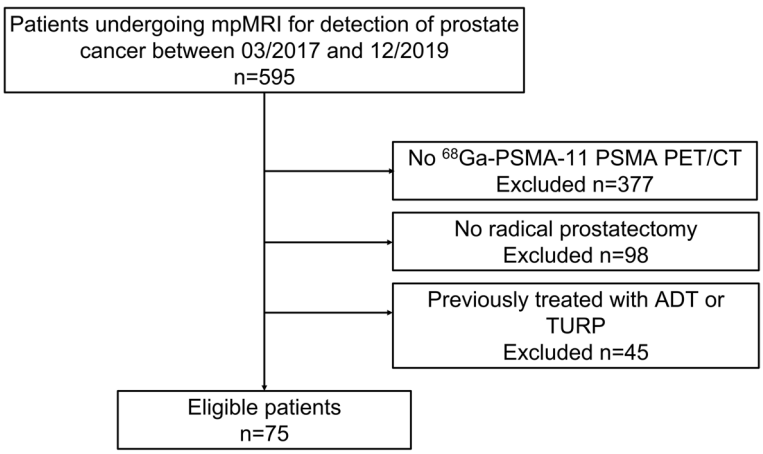


**Fig. 1** Study Flowchart with excluded patients and reasons for exclusion

no radical prostatectomy within 3 months after both $^{68}$ Ga-PSMA-11 PET/CT and mpMRI; (c) had ADT or TURP before prostatectomy (Fig. 1). There were 75 male patients included in all. The Ethics Committee of the Drum Tower Hospital (2017–147-01) had approved the study and all patients had signed informed consent.

#### mpMRI examination

Pelvic mpMRI examinations were performed on patients through a 3.0-T MR scanner (Achieva 3.0 T TX, Philips Medical Systems, The Netherlands) using a 16-channel phased-array coil without endorectal coil [23]. Three planes (Transverse/coronal/sagittal) T2-weighted turbo spin-echo images were obtained. Diffusion-weighted imaging (DWI) spin-echo echo-planar images (b-factor 0/800/1500 s/mm2) were also obtained. Apparent diffusion coefficient (ADC) maps were obtained according to the DWI data. Two dedicated radiologists (15 and 8 years of prostate mpMRI experience) who were blind to $^{68}$ Ga-PSMA-11 PET/CT and pathologist results, read all the images of mpMRI. Prostate Imaging Reporting and Data System (PI-RADS) Version 2 [24] was used as the reference to score each lesion. A five-point Likert-type scale (where 1 = absent, 2 = probably absent, 3 = equivocal, 4 = probably present, and 5 = definitively present) was used to rate the probability of ECE (each lesion) [25].

#### $^{68}$Ga-PSMA-11 PET/CT examination

The ITG semi-automated module (Munich, Germany) synthesized the $^{68}$ Ga-PSMA-11 [26]. All patients were intravenously injected with $^{68}$ Ga-PSMA-11 (median, 131.72 MBq, range 130.6–177.6 MBq) one hour before scanning. The scan machines were a uMI 780 PET-CT scanner (United Imaging Healthcare (UIH), Shanghai, China), a CT scan (130 keV, 80 mAs, slice thickness 3.0 mm) and a static emission scan for correcting dead time, scatter and decay that were obtained from the vertex to the proximal legs (three dimensions matrix 200 × 200). Two dedicated nuclear medicine physicians (13 and 8 years of PET/CT experience) who were blind to mpMRI and pathologist results, read all the images of $^{68}$ Ga-PSMA-11 PET/CT. A miPSMA expression score (MI-ES) [27] was used as the reference to score each lesion. A five-point Likert-type scale (where 1 = absent, 2 = probably absent, 3 = equivocal, 4 = probably present, and 5 = definitively present) was used to rate the probability of ECE (each lesion) [25].

#### Image evaluation

The evaluation of ECE for mpMRI was subjective but guided by the features of PI-RADS, version 2 [24]. The criteria were listed as follows: 1. The recto prostatic angle was obliterated. 2.The interface of the tumor-capsule was greater than 1.0 cm. 3. The tumor extended directly or invaded the bladder wall. 4. The contour of the prostate gland was angulated or spiculate. The evaluation of ECE for $^{68}$ Ga-PSMA-11 PET/CT was also subjective and the criteria were listed as follows: 1. The accumulation of $^{68}$ Ga-PSMA-11 was outside of the prostate capsule. 2. The interface of the tumor-capsule was greater than 1.0 cm.3. The rectoprostatic angle was obliterated. 4. The contour of the prostate gland was angulated or spiculate. For evaluation of ECE, the scale of mpMRI + PET/CT was acquired by the scale of mpMRI plus the scale of $^{68}$ Ga-PSMA-11 PET/CT.

#### Whole mount pathological data

According to the Stanford Protocol [28], the whole-mount tissue was first fixed in 10% formalin, and then paraffin embedded. After that, the tissue was microtome cut into 4 mm slices and then stained with hematoxylin–eosin. We scanned the whole mount histology by NanoZoomer Digital Pathology, Shizuoka, Japan. Two dedicated genitourinary pathologists (15 and 9 years of experience) who were blind to mpMRI and.$^{68}$ Ga-PSMA-11 PET/CT results, read all the pathologic images according to the 2014 International Society of Urological Pathology (ISUP) modified criteria for prostate cancer [29].

#### Image mark and analysis

According to the slice number, we could match the images of the prostate at the same level. We used green color to draw the border of the prostate. In the images of mpMRI or $^{68}$ Ga-PSMA-11 PET/CT, we depicted the lesions in blue. As previously stated, the five-point Likert-type scale was subjective but guided by the features mentioned above [25]. In pathologic images, we depicted the lesions in red (Fig. 3). The final histological specimen results were the gold standard for analyzing image results.

#### Statistical analysis

All statistical analyses were performed using SPSS Statistics, version 26.0 (IBM Corp., Armonk, NY, USA). The diagnostic performances of ECE on mpMRI, $^{68}$ Ga-PSMA-11 PET/CT and mpMRI + PET/CT were evaluated according to the receiver operating characteristics (ROC) curves. Area under the curves (AUCs) and 95% CIs were calculated as proposed by Obuchowski [30]. Logistic generalized estimating equation models were used to estimate sensitivities, specificities and CIs [31–33]. A net reclassification improvement (NRI) was used to compare the images with the calculated cutoff [34]. The Kappa test was used to evaluate the prediction ability [35]. The $\chi 2$ test was performed for categorical

variables. The Mann–Whitney U test was performed for continuous variables. The univariate logistic regression analysis was conducted for all parameters and the multivariate logistic regression analysis was conducted for significant parameters. Two-sided $P<0.05$ was statistically significant.

## Results

### Patient characteristics

There were 75 patients eligible with the characteristics summarized in Table 1. The median age of the patients was 69 years (range, 55–84 years). The median interval time between mpMRI and radical prostatectomy was 24 days (range 2–57). The median interval time between $^{68}$ Ga-PSMA-11 PET/CT and radical prostatectomy was 9 days (range 1–79). According to the histologic examination, 48.5% (50 of 103) of the regions were positive for ECE among 64% (48 of 75) of the patients.

### Diagnostic performance for the detection of ECE

The ROC curves of ECE region-specific analyses are illustrated in Fig. 2 with AUC and 95% CI for each image shown in Table 2. The AUC of mpMRI + PET/CT improved ECE diagnosis comparing to that of mpMRI alone (ΔAUC = 0.101; 95% CI, 0.0148 to 0.1860; $p<0.05$). However, there was no significant difference in AUC between mpMRI + PET/CT and $^{68}$ Ga-PSMA-11 PET/CT (ΔAUC = 0.047; 95% CI, -0.0052 to 0.0992; $p=0.08$). Besides, there was no significant difference in AUC between mpMRI and $^{68}$ Ga-PSMA-11 PET/CT (ΔAUC = 0.053; 95% CI, -0.0690 to 0.1760; $p=0.39$).

Table 2 also shows the Youden-selected threshold, sensitivity and specificity for each image. The cutoff of mpMRI, $^{68}$ Ga-PSMA-11 PET/CT and mpMRI + PET/CT calculated by the Youden-selected threshold and the actual diagnostic results are listed in Table 2. The sensitivity of mpMRI + PET/CT was higher both than mpMRI and $^{68}$ Ga-PSMA-11 PET/CT($p<0.05$ and $p<0.05$), with no sacrifice on specificity ($p=0.34$ and $p=0.50$). There was no significant difference in sensitivity and specificity between mpMRI and $^{68}$ Ga-PSMA-11 PET/CT ($p=0.17$ and $p=0.72$). Compared with mpMRI, mpMRI + PET/CT had a positive NRI (NRI 16.6%, $P=0.051$) with the calculated cutoff (Supplemental Table 1).

Dividing the lesions into PI-RADS 1–3 and PI-RADS 4–5, the ROC curves and AUC of ECE (95% CI) are shown in Fig. 2 and Table 2. In the group of PI-RADS 1–3, there was no significant difference in AUC between mpMRI and $^{68}$ Ga-PSMA-11 PET/CT, mpMRI + PET/CT and mpMRI, mpMRI + PET/CT and $^{68}$ Ga-PSMA-11 PET/CT (ΔAUC = 0.032; 95% CI, -0.2360 to 0.2990; $p=0.82$, ΔAUC = 0.032; 95% CI, -0.1510 to 0.2140; $p=0.73$, ΔAUC = 0.063; 95% CI, -0.0432 to 0.1700; $p=0.24$). In the group of PI-RADS 4–5, the AUC of mpMRI + PET/CT improved ECE diagnosis compared to that of mpMRI alone (ΔAUC = 0.181; 95% CI, 0.0660 to 0.2950; $p<0.01$). However, there was no significant difference for AUC between mpMRI and $^{68}$ Ga-PSMA-11 PET/CT, mpMRI + PET/CT and $^{68}$ Ga-PSMA-11 PET/CT (ΔAUC = 0.145; 95% CI, -0.0041 to 0.2940; $p=0.06$, ΔAUC = 0.036; 95% CI, -0.0329 to 0.1040; $p=0.31$). For further exploration, the NRIs were analyzed and listed in Supplemental Table 1. Compared to mpMRI, mpMRI + PET/CT showed that lesions with PI-RADS 4–5 had a significant improvement (36.1%, $p<0.001$) while lesions with PI-RADS 1–3 had no significant

**Table 1** Baseline Features of the Included Cases ($n=75$) – all underwent mpMRI and $^{68}$ Ga-PSMA-11 PET/CT and Radical Prostatectomy

| Characteristics | Value |
|---|---|
| Age (years), median (range) | 69 (55–84) |
| Initial PSA (ng/dL), median (range) | 14.20 (4.15–120.00) |
| [a]Gleason score, n (%) | |
| 3 + 3 = 6 | 4 (5.3) |
| 3 + 4 = 7 | 27 (36.0) |
| 4 + 3 = 7 | 22 (29.3) |
| 8 point | 11 (14.7) |
| 9–10 point | 11 (14.7) |
| pT stage, n (%) | |
| 2 | 27 (36.0) |
| 3 | 48 (64.0) |
| [a]PI-RADS, n (%) | |
| 3 | 29 (38.7) |
| 4–5 | 46 (61.3) |
| [a]MI-ES, n (%) | |
| 1 | 7 (9.3) |
| 2 | 35 (46.7) |
| 3 | 33 (44.0) |
| [a]ADCmean (μm2 /s), median (range) | 725 (444–1155) |
| [a]SUVmax, median (range) | 14.23 (5.54–90.34) |
| Percentage of positive core at TB (%), median(range) | 36 (7–100) |
| ISUP Gleason score at TB, n (%) | |
| 1 | 13 (17.3) |
| 2 | 14 (18.7) |
| 3 | 9 (12.0) |
| 4 | 27 (36.0) |
| 5 | 12 (16.0) |

*mpMRI* multiparametric magnetic resonance imaging, *PET/CT* positron emission tomography computed tomography, *PSA* prostate-specific antigen, *ISUP* International Society of Urological Pathology, *TB* targeted biopsy, *PI-RADS* Prostate Imaging Reporting and Data System, *MI-ES* a miPSMA expression score, *ADCmean* average apparent diffusion coefficient, *SUVmax* maximum standardized uptake value

[a] For patients with multifoci, the data are based on index lesions

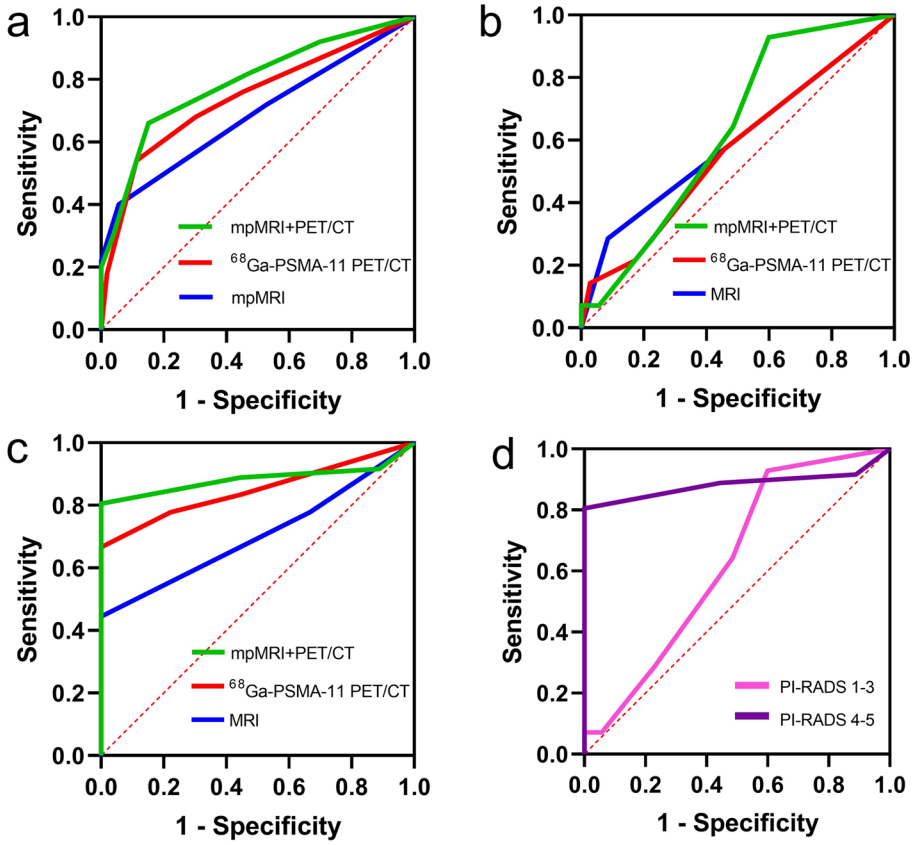


**Fig. 2** Receiver operating characteristics (ROC) analyses. **a** ROC analyses of mpMRI, $^{68}$ Ga-PSMA-11 PET/CT and mpMRI + PET/CT for the detection of ECE of all the lesions; **b** ROC analyses of mpMRI, $^{68}$ Ga-PSMA-11 PET/CT and mpMRI + PET/CT for the detection of ECE of lesions PI-RADS 1–3; **c** ROC analyses of mpMRI, $^{68}$ Ga-PSMA-11 PET/CT and mpMRI + PET/CT for the detection of ECE of lesions PI-RADS 4–5; **d** ROC analyses of lesions PI-RADS 1–3 and PI-RADS 4–5 for the detection of ECE by mpMRI + PET/CT

improvement (12.9%, $p = 0.223$). The sensitivity of mpMRI + PET/CT was higher than mpMRI in lesions with PI-RADS 4–5 ($p < 0.05$) (Table 2).

Figure 3 shows examples of mpMRI and $^{68}$ Ga-PSMA-11 PET/CT results. Figure 3 shows a case of false-positive ECE mpMRI + PET/CT with PI-RADS 3.

### Univariable and multivariable logistic regression for prediction of T staging

Table 3 showed that compared to patients in T2, patients in T3 had a higher initial prostate-specific antigen (PSA), a larger percentage of the positive core at targeted biopsy (TB), higher ISUP Gleason score at TB and a higher scale in the evaluation of ECE by mpMRI + PET/CT. Table 4 showed the results of univariable and multivariable logistic regression for the prediction of T staging. In univariable analysis, initial PSA, percentage of positive core at TB, ISUP Gleason score at TB and mpMRI + PET/CT were significantly associated with T staging. Multivariable logistic regression analysis demonstrated that only mpMRI + PET/CT (OR = 11.337; 95% CI: 3.088 – 41.916; $p < 0.001$) was an independent predictor of T staging.

### Prediction of T staging by mpMRI + PET/CT

Because mpMRI + PET/CT had better performance in patients with PI-RADS 4–5 lesions, we used mpMRI + PET/CT to predict T staging. There were 46 patients enrolled. The cutoffs of ECE were 5. 40 of 46 (87.0%) patients have correct prediction. The κ statistic was 0.70, $p < 0.01$, which indicated a fair consistency (Supplemental Table 2).

## Discussion

To our knowledge, this study is the first to use mpMRI + PET/CT to predict the T staging in prostate cancer patients. The role of mpMRI + PET/CT as an independent predictor of T staging has never been demonstrated before. Based on the mpMRI + PET/CT's improvement in the detection of ECE compared to mpMRI, especially in PI-RADS 4–5, we found that T staging might have the considerable consistency

**Table 2** Diagnostic Accuracies for ECE Using mpMRI, $^{68}$ Ga-PSMA-11 PET/CT and MRI + PET/CT compared to Final Histology

| | | mpMRI | $^{68}$ Ga-PSMA-11 PET/CT | mpMRI + PET/CT |
|---|---|---|---|---|
| PI-RADS 1–5 | | | | |
| AUC (95%CI) | | 0.69 (0.58–0.79)* | 0.74 (0.64–0.84) | 0.79 (0.70–0.88)* |
| Youden-selected threshold | | 3 | 4 | 5 |
| Sensitivity, %, at threshold (95%CI) | | 40 (28–54)* | 54 (40–67)† | 66 (52–78) *† |
| Specificity, %, at threshold (95%CI) | | 94 (85–98) | 89 (77–95) | 85 (73–92) |
| ECE | Positive | 20 | 27 | 33 |
| | Negative | 30 | 23 | 17 |
| None-ECE | Positive | 3 | 6 | 8 |
| | Negative | 50 | 47 | 45 |
| PI-RADS 1–3 | | | | |
| AUC (95%CI) | | 0.60 (0.41–0.78) | 0.56 (0.38–0.74) | 0.62 (0.47–0.79) |
| Youden-selected threshold | | 3 | 3 | 3 |
| Sensitivity, %, at threshold (95%CI) | | 28 (12–55) | 57 (32–79) | 92 (68–100) |
| Specificity, %, at threshold (95%CI) | | 91 (78–97) | 54 (38–70) | 40 (26–56) |
| ECE | Positive | 4 | 6 | 13 |
| | Negative | 10 | 8 | 1 |
| None-ECE | Positive | 3 | 12 | 21 |
| | Negative | 32 | 23 | 14 |
| PI-RADS 4–5 | | | | |
| AUC (95%CI) | | 0.70 (0.57–0.84)* | 0.85 (0.75–0.95) | 0.88 (0.79–0.98)* |
| Youden-selected threshold | | 3 | 4 | 5 |
| Sensitivity, %, at threshold (95%CI) | | 44 (30–60)* | 66 (50–80) | 80 (65–90)* |
| Specificity, %, at threshold (95%CI) | | 100 (82–100) | 100 (82–100) | 100 (82–100) |
| ECE | Positive | 16 | 24 | 29 |
| | Negative | 20 | 12 | 7 |
| None-ECE | Positive | 0 | 0 | 0 |
| | Negative | 18 | 18 | 18 |

*PI-RADS* Prostate Imaging Reporting and Data System, *AUC* area under the curve, *CI* confidence interval, *mpMRI* multiparametric magnetic resonance imaging, *PET/CT* positron emission tomography computed tomography, *ECE* extracapsular extension, *mpMRI + PET/CT* combination of $^{68}$ Ga-PSMA-11 PET/CT and mpMRI

* mpMRI versus mpMRI + PET/CT, $p < 0.05$

† PET/CT versus mpMRI + PET/CT, $p < 0.05$

between mpMRI + PET/CT and final pathology. By using mpMRI + PET/CT for primary detection of prostate cancer, we can determine the mode and scope of surgery according to the predicted results, which is conducive to clinical work [17].

In our study, we wanted to further explore the relationship between $^{68}$ Ga-PSMA-11 PET/CT and final pathology at first. However, $^{68}$ Ga-PSMA-11 PET/CT also had some disabilities like image fusion deviation or differences in concentration, action time, individual metabolic of tracers and etc. To fill these gaps, we included mpMRI and clinical features to improve the predictive power for final pathology [5]. Through a series of analyses, we found that mpMRI + PET/CT had a fair performance in the prediction of T staging.

For economic considerations, mpMRI + PET/CT may be better than $^{68}$ Ga-PSMA-11 PET/MRI. For patients with PI-RADS 1–3, $^{68}$ Ga-PSMA-11 PET/CT or PET/MRI is not a prerequisite for early staging [25]. Although mpMRI + PET/CT can improve the detection of csPCa for lesions with PI-RADS 3, we should still adopt a prudent policy in patients with lesions with PI-RADS 3, especially when the ECE is positive for $^{68}$ Ga-PSMA-11 PET/CT but negative for mpMRI [5]. Compared to $^{68}$ Ga-PSMA-11 PET/CT, mpMRI costs less and has less damage to human health. We chose the right time to use the proper imaging tools, so that they can have the maximum value in clinical diagnosis. Beyond that, patients' suffering and medical expenses should be reduced for humanitarian reasons.

For more accurate prediction of T staging, mpMRI + PET/CT should be included in the Nomogram with more clinical features for prediction of ECE [36, 37]. With the improvement of prediction ability with comprehensive clinical information, miTNM will play a greater value in prostate cancer diagnosis [27]. Nowadays, it still

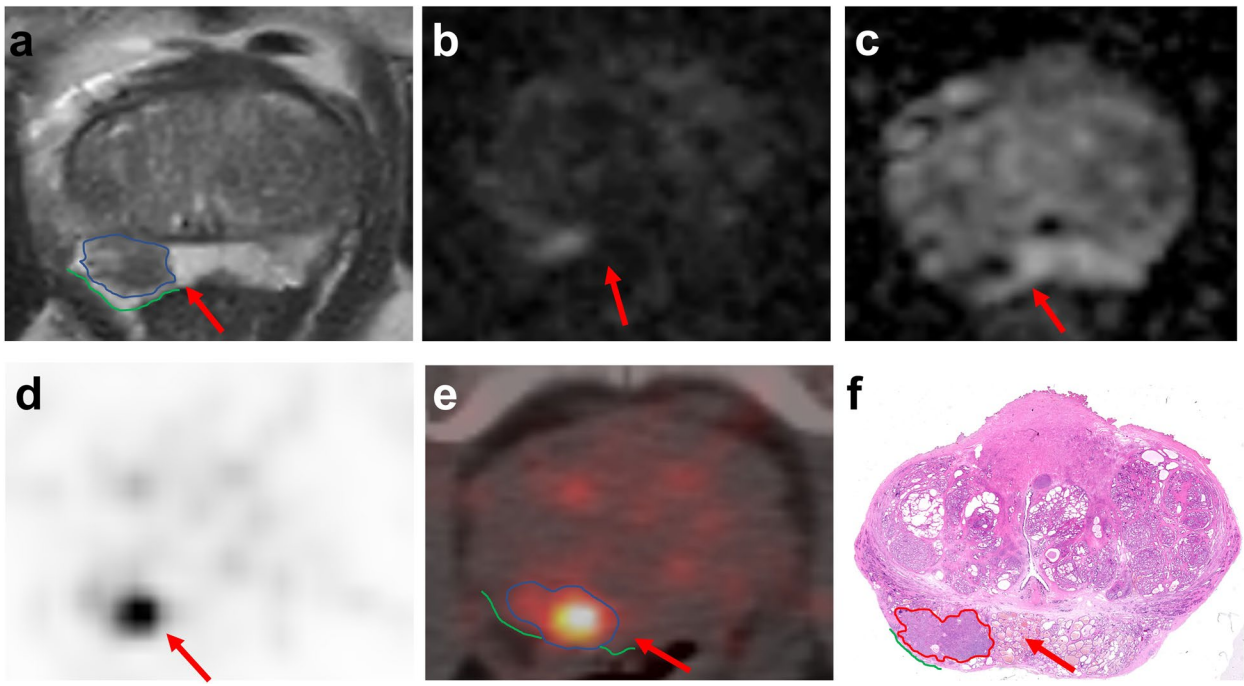


**Fig. 3** The images of a 67-year-old patient with prostate-specific antigen of 5.46 ng/ml. **a** Transverse T2-weighted images on MRI showed a lesion in the right peripheral zone (red arrow). **b** DWI with b1500 shows a moderately high signal on the edge of right peripheral zone (red arrow). **c** ADC map showed a moderate hypo intensity on the edge of right peripheral zone (red arrow). All the finding results in a PI-RADS 3. **d, e** PET showed great intense focal uptake on the right peripheral zone (red arrow), which is equal to the parotid gland, resulting in an MI-ES 3. Readers rated the images from mpMRI as negative for extraprostatic extension (Likert scale points = 2), whereas they rated the images from.[68] Ga-PSMA-11 PET/CT and mpMRI + PET/CT as positive for extraprostatic extension (Likert scale points = 4 and 6). **f** Whole mount histology confirms the tumor in the right peripheral zone without extraprostatic extension (red arrow)

lacks favorable evidence that $^{68}$ Ga-PSMA-11 PET/MRI has better performance than $^{68}$ Ga-PSMA-11 PET/CT. $^{68}$ Ga-PSMA-11 PET/MRI has a long inspection time and higher cost. Except for that, most patients would conduct mpMRI before $^{68}$ Ga-PSMA-11 PET/CT or $^{68}$ Ga-PSMA-11 PET/MRI, which means that $^{68}$ Ga-PSMA-11 PET/MRI would have a certain degree of repeated inspection.

As highly sensitive imaging diagnostic tools, the sensitivity and specificity of $^{68}$ Ga-PSMA-11 PET/CT were, respectively, 90.0% and 90.9% for ECE [38]. Besides, $^{68}$ Ga-PSMA-11 PET/MRI had an increased sensitivity for ECE compared to mpMRI (69% vs 46%, $p = 0.04$) [25]. In our study, the mpMRI + PET/CT also had higher sensitivity in ECE than mpMRI (66% vs 40%, $p < 0.05$). However, specificity had no increase or even slight reduction, especially in PI-RADS 3. It is likely due to an image fusion error. In future research, we want to find the influence factors of specificity reduction in $^{68}$ Ga-PSMA-11 PET/CT or mpMRI + PET/CT.

$^{68}$ Ga-PSMA-11 PET/CT has the potential advantage in prostate cancer primary staging and the combination of mpMRI had higher accuracy [39]. In our study, we combined mpMRI and $^{68}$ Ga-PSMA-11 PET/CT to predict T staging in PI-RADS 4–5 (87.0%, 0.70, $p < 0.01$). The result demonstrated that we could have more accurate local staging prior to surgery.

The limitations of our study are listed as follows: 1. Selection bias: all patients underwent surgery in order to obtain pathological specimens, hence, no negative or low risk patients were included. 2.Limited samples: our study enrolled 75 patients which might have a certain influence on the reliability of results. But for a variety of reasons, there were only a handful of patients who met all the requirements.3. Heterogeneity: because of this study's retrospective nature, there were many variables not under full control, including but not limited to the examination duration and the examination intervals.

## Conclusions

Our study verifies that mpMRI + PET/CT can improve ECE diagnosis compared to mpMRI, especially in prostate cancer patients with PI-RADS 4–5 lesions. The diagnosis of mpMRI + PET/CT was an independent predictor ($p < 0.001$) in logistic regression analysis. The prediction power of T staging in PI-RADS 4–5 prostate cancer by mpMRI + PET/CT was moderate. These results may help clinical decisions on primary staging for prostate cancer diagnosis before surgical operation in a more economical way.

**Table 3** Clinical and imaging characteristics of patients ($n=75$) with T2 and T3 in final pathology

| | T2 (27, 36.0%) | T3 (48, 64.0%) | *p* |
|---|---|---|---|
| Age (years), median (range) | 69 (58–82) | 68 (55–84) | 0.868 |
| Initial PSA (ng/dL), median (range) | 9.87 (4.15–60.17) | 15.06 (5.42–120) | **0.016** |
| Percentage of positive core at TB (%), median (range) | 28.6 (7.1–81.2) | 41.7 (7.1–100) | **0.031** |
| ISUP Gleason score at TB, n (%) | | | **0.032** |
| 1 | 8 (29.6) | 5 (10.4) | |
| 2 | 8 (29.6) | 6 (12.5) | |
| 3 | 3 (11.1) | 6 (12.5) | |
| 4 | 6 (22.2) | 21 (43.8) | |
| 5 | 2 (7.4) | 10 (20.8) | |
| mpMRI + PET/CT, n (%) | | | |
| scale | | | **0.013** |
| 2 | 1 (3.7) | 3 (6.3) | |
| 3 | 9 (33.3) | 6 (12.5) | |
| 4 | 12 (44.4) | 7 (14.6) | |
| 5 | 1 (3.7) | 6 (12.5) | |
| 6 | 3 (11.1) | 12 (25.0) | |
| 7 | 1 (3.7) | 4 (8.3) | |
| 8 | 0 (0) | 3 (6.25) | |
| 9 | 0 (0) | 5 (10.4) | |
| 10 | 0 (0) | 2 (4.16) | |
| Diagnosis | | | **< 0.001** |
| Positive | 5 | 32 | |
| Negative | 22 | 16 | |

*PSA* prostate-specific antigen, *ISUP* International Society of Urological Pathology, *TB* targeted biopsy, *mpMRI + PET/CT* combination of $^{68}$ Ga-PSMA-11 PET/CT and mpMRI

Significant *P* values were presented in bold text

**Table 4** Univariable and multivariable logistic regression analysis of possible predictors for distinguishing patients ($n=75$) between T2 and T3 in final pathology

| Parameters | Univariable logistic regression | | | Multivariable logistic regression | | |
|---|---|---|---|---|---|---|
| | OR | 95% CI | *p* | OR | 95% CI | *p* |
| Age (years), median (range) | 1.000 | 0.928 – 1.079 | 0.990 | | | |
| Initial PSA (ng/dL), median (range) | 1.029 | 1.001 – 1.058 | **0.042** | 1.027 | 0.992 – 1.064 | 0.136 |
| Percentage of positive core at TB (%), median (range) | 1.029 | 1.001 – 1.057 | **0.041** | 0.637 | 0.972 – 1.048 | 0.637 |
| ISUP Gleason score at TB, n (%) | | | **0.044** | | | 0.234 |
| 1 vs. 2 | 1.200 | 0.257 – 5.593 | 0.816 | 0.759 | 0.105 – 5.473 | 0.784 |
| 1 vs. 3 | 3.200 | 0.540 – 18.980 | 0.200 | 2.168 | 0.250 – 18.833 | 0.483 |
| 1 vs. 4 | 5.600 | 1.328 – 23.620 | **0.019** | 2.755 | 0.425 – 17.868 | 0.288 |
| 1 vs. 5 | 8.000 | 1.215 – 52.693 | **0.031** | 9.842 | 0.789 – 122.734 | 0.076 |
| mpMRI + PET/CT | | | | | | |
| Negative vs. Positive | 8.800 | 2.810 – 27.557 | **< 0.001** | 11.377 | 3.088 – 41.916 | **< 0.001** |

*PSA* prostate-specific antigen, *ISUP* International Society of Urological Pathology, *TB* targeted biopsy, *mpMRI + PET/CT* combination of $^{68}$ Ga-PSMA-11 PET/CT and mpMRI, *OR* odds ratio, *CI* confidence intervals

Significant *P* values were presented in bold text

**Abbreviations**

| | |
|---|---|
| mpMRI | Multiparametric magnetic resonance imaging |
| mpMRI + PET/CT | Combination of $^{68}$ Ga-PSMA-11 PET/CT and mpMRI |
| csPCa | Clinically significant prostate cancer |
| AJCC | American Joint Committee on Cancer |
| ECE | Extracapsular extension |
| PET | Positron emission tomography |
| CT | Computed tomography |
| DWI | Diffusion-weighted imaging |
| ADC | Apparent diffusion coefficient |
| ISUP | International Society of Urological Pathology |
| PI-RADS | Prostate Imaging Reporting and Data System |
| MI-ES | MiPSMA expression score |
| ROC | Receiver operating characteristics |
| AUC | Area under the curve |
| NRI | Net reclassification improvement |
| PSA | Prostate-specific antigen |
| TB | Targeted biopsy |

## Supplementary Information

The online version contains supplementary material available at https://doi.org/10.1186/s12894-023-01376-6.

**Additional file 1: Supplemental Table 1.** Diagnostic Changement for the Detection of ECE by mpMRI+PET/CT compared to mpMRI.

**Additional file 2: Supplemental Table 2.** Prediction Consistency of T stage in PI-RADS 4-5 Prostate Cancer by mpMRI+PET/CT.

**Acknowledgements**
Not applicable.

**Authors' contributions**
HQG, QZ, SWZ, TSL, JG, MXC and YZD conceived and designed the analysis. YZD, CHM and QBD participated in the analysis and drafted the manuscript. WFL, JYS, SMZ, and FW contributed to the sample collection and interpretation of the data. All authors read and approved the final manuscript.

**Funding**
This work was funded by the National Natural Science Foundation of China (82072822, 81802535, 81772710, 81972388), China postdoctoral fund (223427), Nanjing Medical Science and Technique Development Foundation (YKK 18064). This work was also supported by the Project of Invigorating Health Care through Science, Technology and Education Jiangsu Provincial Key Medical Discipline (ZDXKB2016014).

**Availability of data and materials**
The datasets used and/or analyzed during the current study are available from the corresponding author upon reasonable request.

## Declarations

**Ethics approval and consent to participate**
The study was approved by the Ethical Committee of Nanjing Drum Tower Hospital, Medical School of Nanjing University. (2017–147-01) Informed consent was obtained from all individual participants included in the study. The study was conducted in accordance with the Declaration of Helsinki.

**Consent for publication**
Not applicable.

**Competing interests**
The authors declare no competing interests.

**Author details**
[1]Department of Urology, Nanjing Drum Tower Hospital, Affiliated Hospital of Medical School, Nanjing University, 321 Zhongshan Road, Nanjing 210008, Jiangsu, China. [2]Department of Urology, Drum Tower Hospital Clinical College of Nanjing Medical University, 321 Zhongshan Road, Nanjing 210008, Jiangsu, China. [3]Department of Nuclear Medicine, Nanjing First Hospital, Nanjing Medical University, 68 Changle Road, Nanjing 210006, Jiangsu, China.

Received: 25 April 2023 Accepted: 23 November 2023
Published online: 11 December 2023

**References**

1. Pomykala KL, Farolfi A, Hadaschik B, Fendler WP, Herrmann K. Molecular imaging for primary staging of prostate cancer. Semin Nucl Med. 2019;49:271–9. https://doi.org/10.1053/j.semnuclmed.2019.02.004.
2. Sung H, Ferlay J, Siegel RL, Laversanne M, Soerjomataram I, Jemal A, et al. Global cancer statistics 2020: GLOBOCAN estimates of incidence and mortality worldwide for 36 cancers in 185 countries. CA Cancer J Clin. 2021. https://doi.org/10.3322/caac.21660.
3. Hofman MS, Lawrentschuk N, Francis RJ, Tang C, Vela I, Thomas P, et al. Prostate-specific membrane antigen PET-CT in patients with high-risk prostate cancer before curative-intent surgery or radiotherapy (proPSMA): a prospective, randomised, multicentre study. Lancet. 2020;395:1208–16. https://doi.org/10.1016/s0140-6736(20)30314-7.
4. Bjurlin MA, Carroll PR, Eggener S, Fulgham PF, Margolis DJ, Pinto PA, et al. Update of the standard operating procedure on the use of multiparametric magnetic resonance imaging for the diagnosis, staging and Management of Prostate Cancer. J Urol. 2020;203:706–12. https://doi.org/10.1097/ju.0000000000000617.
5. Chen M, Zhang Q, Zhang C, Zhao X, Marra G, Gao J, et al. Combination of (68)Ga-PSMA PET/CT and multiparametric MRI improves the detection of clinically significant prostate cancer: a lesion-by-lesion analysis. J Nucl Med. 2019;60:944–9. https://doi.org/10.2967/jnumed.118.221010.
6. Cheng L, Montironi R, Bostwick DG, Lopez-Beltran A, Berney DM. Staging of prostate cancer. Histopathology. 2012;60:87–117. https://doi.org/10.1111/j.1365-2559.2011.04025.x.
7. Amin MB, Edge SB, Greene FL. AJCC Cancer Staging Manual 8. Cham: Springer; 2017.
8. Wiegel T, Bartkowiak D, Bottke D, Bronner C, Steiner U, Siegmann A, et al. Adjuvant radiotherapy versus wait-and-see after radical prostatectomy: 10-year follow-up of the ARO 96–02/AUO AP 09/95 trial. Eur Urol. 2014;66:243–50. https://doi.org/10.1016/j.eururo.2014.03.011.
9. Mottet N, Bellmunt J, Bolla M, Briers E, Cumberbatch MG, De Santis M, et al. EAU-ESTRO-SIOG guidelines on prostate cancer. Part 1: screening, diagnosis, and local treatment with curative intent. Eur Urol. 2017;71:618–29. https://doi.org/10.1016/j.eururo.2016.08.003.
10. Bill-Axelson A, Holmberg L, Garmo H, Taari K, Busch C, Nordling S, et al. Radical prostatectomy or watchful waiting in prostate cancer - 29-year follow-up. N Engl J Med. 2018;379:2319–29. https://doi.org/10.1056/NEJMoa1807801.
11. Schröder FH, Hermanek P, Denis L, Fair WR, Gospodarowicz MK, Pavone-Macaluso M. The TNM classification of prostate cancer. Prostate Suppl. 1992;4:129–38. https://doi.org/10.1002/pros.2990210521.
12. Fukunaga A, Maejima A, Shinoda Y, Matsui Y, Komiyama M, Fujimoto H, et al. Prognostic implication of staging of seminal vesicle invasion in patients with prostatic adenocarcinoma after prostatectomy. Int J Urol. 2021;28:1039–45. https://doi.org/10.1111/iju.14643.
13. Afshar-Oromieh A, Haberkorn U, Eder M, Eisenhut M, Zechmann CM. [68Ga]Gallium-labelled PSMA ligand as superior PET tracer for the diagnosis of prostate cancer: comparison with 18F-FECH. Eur J Nucl Med Mol Imaging. 2012;39:1085–6. https://doi.org/10.1007/s00259-012-2069-0.
14. Afshar-Oromieh A, Malcher A, Eder M, Eisenhut M, Linhart HG, Hadaschik BA, et al. PET imaging with a [68Ga]gallium-labelled PSMA ligand for the diagnosis of prostate cancer: biodistribution in humans and first evaluation of tumour lesions. Eur J Nucl Med Mol Imaging. 2013;40:486–95. https://doi.org/10.1007/s00259-012-2298-2.
15. Coenen HH, Gee AD, Adam M, Antoni G, Cutler CS, Fujibayashi Y, et al. International consensus radiochemistry nomenclature guidelines. Nuklearmedizin. 2018;57:40–1. https://doi.org/10.1055/s-0038-1636563.
16. Perera M, Papa N, Roberts M, Williams M, Udovicich C, Vela I, et al. Gallium-68 prostate-specific membrane antigen positron emission

tomography in advanced prostate cancer-updated diagnostic utility, sensitivity, specificity, and distribution of prostate-specific membrane antigen-avid lesions: a systematic review and meta-analysis. Eur Urol. 2020;77:403–17. https://doi.org/10.1016/j.eururo.2019.01.049.
17. Lopci E, Saita A, Lazzeri M, Lughezzani G, Colombo P, Buffi NM, et al. (68) Ga-PSMA positron emission tomography/computerized tomography for primary diagnosis of prostate cancer in men with contraindications to or negative multiparametric magnetic resonance imaging: a prospective observational study. J Urol. 2018;200:95–103. https://doi.org/10.1016/j.juro.2018.01.079.
18. Ahmadzadehfar H, Essler M. Prostate-specific membrane antigen imaging: a game changer in prostate cancer diagnosis and therapy planning. Eur Urol. 2020;77:418–9. https://doi.org/10.1016/j.eururo.2019.02.028.
19. Schoots IG, Roobol MJ, Nieboer D, Bangma CH, Steyerberg EW, Hunink MG. Magnetic resonance imaging-targeted biopsy may enhance the diagnostic accuracy of significant prostate cancer detection compared to standard transrectal ultrasound-guided biopsy: a systematic review and meta-analysis. Eur Urol. 2015;68:438–50. https://doi.org/10.1016/j.eururo.2014.11.037.
20. Stabile A, Giganti F, Rosenkrantz AB, Taneja SS, Villeirs G, Gill IS, et al. Multiparametric MRI for prostate cancer diagnosis: current status and future directions. Nat Rev Urol. 2020;17:41–61. https://doi.org/10.1038/s41585-019-0212-4.
21. de Rooij M, Hamoen EH, Witjes JA, Barentsz JO, Rovers MM. Accuracy of magnetic resonance imaging for local staging of prostate cancer: a diagnostic meta-analysis. Eur Urol. 2016;70:233–45. https://doi.org/10.1016/j.eururo.2015.07.029.
22. Johnson DC, Raman SS, Mirak SA, Kwan L, Bajgiran AM, Hsu W, et al. Detection of individual prostate cancer foci via multiparametric magnetic resonance imaging. Eur Urol. 2019;75:712–20. https://doi.org/10.1016/j.eururo.2018.11.031.
23. Zhang Q, Wang W, Zhang B, Shi J, Fu Y, Li D, et al. Comparison of free-hand transperineal MPMRI/TRUS fusion-guided biopsy with transperineal 12-core systematic biopsy for the diagnosis of prostate cancer: a single-center prospective study in China. Int Urol Nephrol. 2017;49:439–48. https://doi.org/10.1007/s11255-016-1484-8.
24. Weinreb JC, Barentsz JO, Choyke PL, Cornud F, Haider MA, Macura KJ, et al. PI-RADS prostate imaging - reporting and data system: 2015, version 2. Eur Urol. 2016;69:16–40. https://doi.org/10.1016/j.eururo.2015.08.052.
25. Muehlematter UJ, Burger IA, Becker AS, Schawkat K, Hotker AM, Reiner CS, et al. Diagnostic accuracy of multiparametric MRI versus (68)Ga-PSMA-11 PET/MRI for extracapsular extension and seminal vesicle invasion in patients with prostate cancer. Radiology. 2019;293:350–8. https://doi.org/10.1148/radiol.2019190687.
26. Zhang Q, Zang S, Zhang C, Fu Y, Lv X, Zhang Q, et al. Comparison of (68) Ga-PSMA-11 PET-CT with mpMRI for preoperative lymph node staging in patients with intermediate to high-risk prostate cancer. J Transl Med. 2017;15:230. https://doi.org/10.1186/s12967-017-1333-2.
27. Eiber M, Herrmann K, Calais J, Hadaschik B, Giesel FL, Hartenbach M, et al. Prostate cancer molecular imaging standardized evaluation (PROMISE): proposed miTNM classification for the interpretation of PSMA-ligand PET/CT. J Nucl Med. 2018;59:469–78. https://doi.org/10.2967/jnumed.117.198119.
28. McNeal JE, Haillot O. Patterns of spread of adenocarcinoma in the prostate as related to cancer volume. Prostate. 2001;49:48–57. https://doi.org/10.1002/pros.1117.
29. Epstein JI, Egevad L, Amin MB, Delahunt B, Srigley JR, Humphrey PA. The 2014 International Society of Urological Pathology (ISUP) consensus conference on gleason grading of prostatic carcinoma: definition of grading patterns and proposal for a new grading system. Am J Surg Pathol. 2016;40:244–52. https://doi.org/10.1097/pas.0000000000000530.
30. Obuchowski NA. Nonparametric analysis of clustered ROC curve data. Biometrics. 1997;53:567–78.
31. Zeger SL, Liang KY. Longitudinal data analysis for discrete and continuous outcomes. Biometrics. 1986;42:121–30.
32. Smith PJ, Hadgu A. Sensitivity and specificity for correlated observations. Stat Med. 1992;11:1503–9. https://doi.org/10.1002/sim.4780111108.
33. Genders TS, Spronk S, Stijnen T, Steyerberg EW, Lesaffre E, Hunink MG. Methods for calculating sensitivity and specificity of clustered data: a tutorial. Radiology. 2012;265:910–6. https://doi.org/10.1148/radiol.12120509.
34. Leening MJ, Vedder MM, Witteman JC, Pencina MJ, Steyerberg EW. Net reclassification improvement: computation, interpretation, and controversies: a literature review and clinician's guide. Ann Intern Med. 2014;160:122–31. https://doi.org/10.7326/m13-1522.
35. Hayden JA, van der Windt DA, Cartwright JL, Côté P, Bombardier C. Assessing bias in studies of prognostic factors. Ann Intern Med. 2013;158:280–6. https://doi.org/10.7326/0003-4819-158-4-201302190-00009.
36. Steuber T, Graefen M, Haese A, Erbersdobler A, Chun FKH, Schlom T, et al. Validation of a nomogram for prediction of side specific extracapsular extension at radical prostatectomy. J Urol. 2006;175:939–44. https://doi.org/10.1016/s0022-5347(05)00342-3.
37. Wang L, Hricak H, Kattan MW, Chen HN, Kuroiwa K, Eisenberg HF, et al. Prediction of seminal vesicle invasion in prostate cancer: incremental value of adding endorectal MR imaging to the Kattan nomogram. Radiology. 2007;242:182–8. https://doi.org/10.1148/radiol.2421051254.
38. von Klot CJ, Merseburger AS, Boker A, Schmuck S, Ross TL, Bengel FM, et al. (68)Ga-PSMA PET/CT imaging predicting intraprostatic tumor extent, extracapsular extension and seminal vesicle invasion prior to radical prostatectomy in patients with prostate cancer. Nucl Med Mol Imaging. 2017;51:314–22. https://doi.org/10.1007/s13139-017-0476-7.
39. Kesch C, Vinsensia M, Radtke JP, Schlemmer HP, Heller M, Ellert E, et al. Intraindividual comparison of (18)F-PSMA-1007 PET/CT, multiparametric MRI, and radical prostatectomy specimens in patients with primary prostate cancer: a retrospective. Proof-of-Concept Study J Nucl Med. 2017;58:1805–10. https://doi.org/10.2967/jnumed.116.189233.

## Publisher's Note